Journal of Solid State Chemistry **148,** 119–128 (1999)
Article ID jssc.1999.8391, available online at http://www.idealibrary.com on IDEAL®

Local Structural Perturbations in $HgBa_2CuO_{4+\delta}$

Neil C. Hyatt,* Jason P. Hodges,*,[1] Ian Gameson,* Steve Hull,† and Peter P. Edwards*,[2]

*School of Chemistry, University of Birmingham, Edgbaston, Birmingham, B15 2TT, United Kingdom; and †ISIS Facility, Rutherford Appleton Laboratory, Chilton, Didcot, Oxon, OX11 0QX, United Kingdom

Received May 11, 1999; accepted May 21, 1999

DEDICATED TO PROFESSOR C. N. R. RAO, FRS ON HIS 65TH BIRTHDAY

The high-temperature superconduct?or, $HgBa_2CuO_{4+\delta}$ ($\delta > 0$), is the first and arguably the most simple member of the homologous series of mercury-based cuprates, of general formula $HgBa_2Ca_{n-1}Cu_nO_{2n+2+\delta}$ ($n = 1 \ldots 8$). The presence of interstitial oxygen in the HgO_δ rock salt layer is crucial in controlling the electronic structure of $HgBa_2CuO_{4+\delta}$. Thus, by careful control of the concentration (δ) of interstitial oxygen, one may fine-tune the electronic properties of this material from insulating, through superconducting, to metallic behavior. The local structure adjusts to the presence of interstitial oxygen by displacement of neighboring atoms from their "ideal" positions. We present here a combined powder X-ray and time-of-flight neutron diffraction study of $HgBa_2CuO_{4+\delta}$ (space group *P4/mmm*, lattice parameters $a = 3.8757(1)$ Å and $c = 9.4998(1)$ Å, $\delta = 0.07$). From this conjoint approach (powder X-ray and neutron diffraction) we are able to identify the local structural perturbations and atom displacements arising from the occupany ($\delta = 0.07$) of the interstitial oxygen site in $HgBa_2CuO_{4+\delta}$. © 1999 Academic Press

Key Words: **high-temperature superconductor; powder X-ray diffraction; powder neutron diffraction; structure.**

INTRODUCTION

The mercurocuprate superconductors of the homologous series $HgBa_2Ca_{n-1}Cu_nO_{2n+2+\delta}$ represent the current summit of achievement in the chemistry of high temperature cuprate superconductors (1, 2). The crystal structures of this family of superconductors are composed of rock-salt type $(BaO)_c(HgO_\delta)_o(BaO)_c$ blocks and oxygen-deficient perovskite type $(CuO_2)_o(Ca)_c(CuO_2)_o$ layers, assembled in the stacking sequence

$$\ldots (BaO)_c(HgO_\delta)_o(BaO)_c(CuO_2)_o[(Ca)_c(CuO_2)_o]_{n-1} \ldots,$$

where the subscripts *c* and *o* denote cations at the *center* and *origin* of the structural units, respectively. To date, the $n = 1 \ldots 8$ members of the $HgBa_2Ca_{n-1}Cu_nO_{2n+2+\delta}$ homologous series, have been identified (1, 2).

The role of the interstitial oxygen site in the HgO_δ plane is fundamental in controlling the electronic properties of these materials. Controlling the occupancy (δ) of this interstitial oxygen site allows one to chemically "tune" the electronic properties of the mercurocuprates from insulating, through superconducting, to metallic behavior.

In the present work, we focus on the crystal structure and chemistry of $HgBa_2CuO_{4+\delta}$ (the $n = 1$ member of the $HgBa_2Ca_{n-1}Cu_nO_{2n+2+\delta}$ homologous series) and examine the relaxation of the local crystal structure around the occupied interstitial oxygen site in the HgO_δ plane. A schematic representation of the crystal structure of $HgBa_2CuO_{4+\delta}$ is shown in Fig. 1; the interstitial oxygen site in this material is located at the O3 position with coordinates $(\frac{1}{2}, \frac{1}{2}, 0)$. In $HgBa_2CuO_{4+\delta}$, the superconducting transition temperature, T_c, is related to the occupancy of the interstitial oxygen site by the generalized equation (2)

$$T_c = 97[1 - 190(\delta - \delta_{opt})^2], \qquad [1]$$

where δ_{opt} ($=0.086$) is the occupancy of the interstitial oxygen site which corresponds to the optimum $T_c = 97$ K in $HgBa_2CuO_{4+\delta}$ (1–3).

A consensus has now emerged concerning the general features of the crystal structure of $HgBa_2CuO_{4+\delta}$, shown in Fig. 1. However, this consensus does not encompass the fine details of the crystal structure, and a continuing discussion centers upon three key issues: first, the possible substitution of mercury by copper; second, the possible substitution of mercury by carbon (in the form of the carbonate anion, CO_3^{2-}); and third, the possibility of static displacements of mercury, oxygen, and barium induced by the occupation of the interstitial site in the HgO_δ plane. The experimental evidence for these proposed substitutional defects may be gleaned from an inspection of Table 1, which summarizes

[1]Present address: Argonne National Laboratory, 9700 South Cass Avenue, Argonne, IL 60439.
[2]To whom correspondence should be addressed. E-mail: p.p.edwards@bham.ac.uk.

0022-4596/99 $30.00

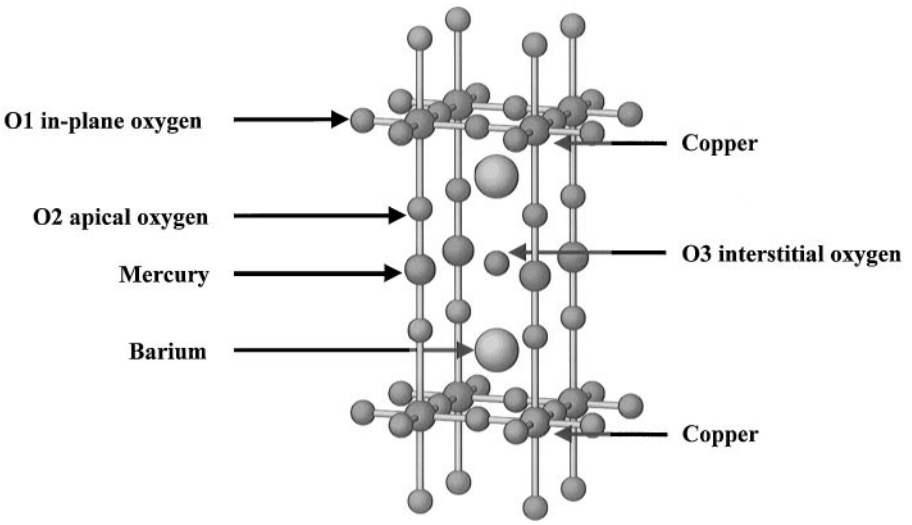

FIG. 1. Schematic representation of the structure of $HgBa_2CuO_{4+\delta}$.

the crystallographic data for $HgBa_2CuO_{4+\delta}$ derived from both published powder neutron (PND) (4–6) and single-crystal X-ray (SXRD) (7) diffraction studies. The high isotropic thermal parameter (B_{iso}) associated with the Hg atom (common to all these studies) has been attributed to a deficiency of scattering at this site, due to the partial substitution of mercury by the lighter elements copper or carbon. Alternatively, the high isotropic thermal parameter associated with the Hg atom may be symptomatic of static displacement of the Hg atom from the ideal (0, 0, 0) position. Notably, the large thermal parameter of the O2 apical oxygen (relative to that of the O1 in-plane oxygen), is also common to all the studies referenced in Table 1, suggesting some static displacement of this oxygen atom, perhaps in association with the proposed displacement of the Hg cation (shown schematically in Fig. 2a). The possible displacement of the O2 oxygen may be coupled with the partial substitution of mercury by copper (shown schematically in Fig. 2b) or carbonate (shown schematically in Fig. 2c). In the case of such a substitutional defect, one would expect

TABLE 1
Survey of Crystallographic Data for $HgBa_2CuO_{4+\delta}$ (from Various Sources)

				Ref. 4	Ref. 5	Ref. 6	Ref. 7
Technique				PND	PND	PND	SXRD[a]
Lattice parameters			a (Å)	3.8829(6)	3.88051(7)	3.8731(1)	3.874(1)
			c (Å)	9.5129(14)	9.5288(3)	9.4829(5)	9.504(9)
Hg	1*a*	(0, 0, 0)	n	1	1	1	1
			B_{iso} (Å^2)	1.3(2)	1.37(5)	1.37(7)	1.37
Ba	2*h*	$(\frac{1}{2}, \frac{1}{2}, z)$	z	0.2988(6)	0.2981(3)	0.2939(4)	0.2991(1)
			n	1	1	1	1
			B_{iso} (Å^2)	0.2(1)	0.80(5)	0.70(8)	0.89
Cu	1*b*	$(0, 0, \frac{1}{2})$	n	1	1	1	1
			B_{iso} (Å^2)	0.2(2)	0.59(5)	0.48(8)	0.72
O1	2*e*	$(0, \frac{1}{2}, \frac{1}{2})$	n	1	1	1	1
			B_{iso} (Å^2)	0.4(1)	0.82(5)	0.64(8)	1.02
O2	2*g*	(0, 0, *z*)	z	0.2073(1)	0.2076(3)	0.2100(4)	0.2092(6)
			n	1	1	1	1
			B_{iso} (Å^2)	1.0(1)	1.42(5)	1.28(8)	1.72
O3	1*c*	$(\frac{1}{2}, \frac{1}{2}, 0)$	n	0.063(14)	0.18(1)	0.23(3)	0.06(6)
			B_{iso} (Å^2)	1.2	1.6	2.79(9)	1.84

[a]No standard deviations are given for isotropic thermal parameters.

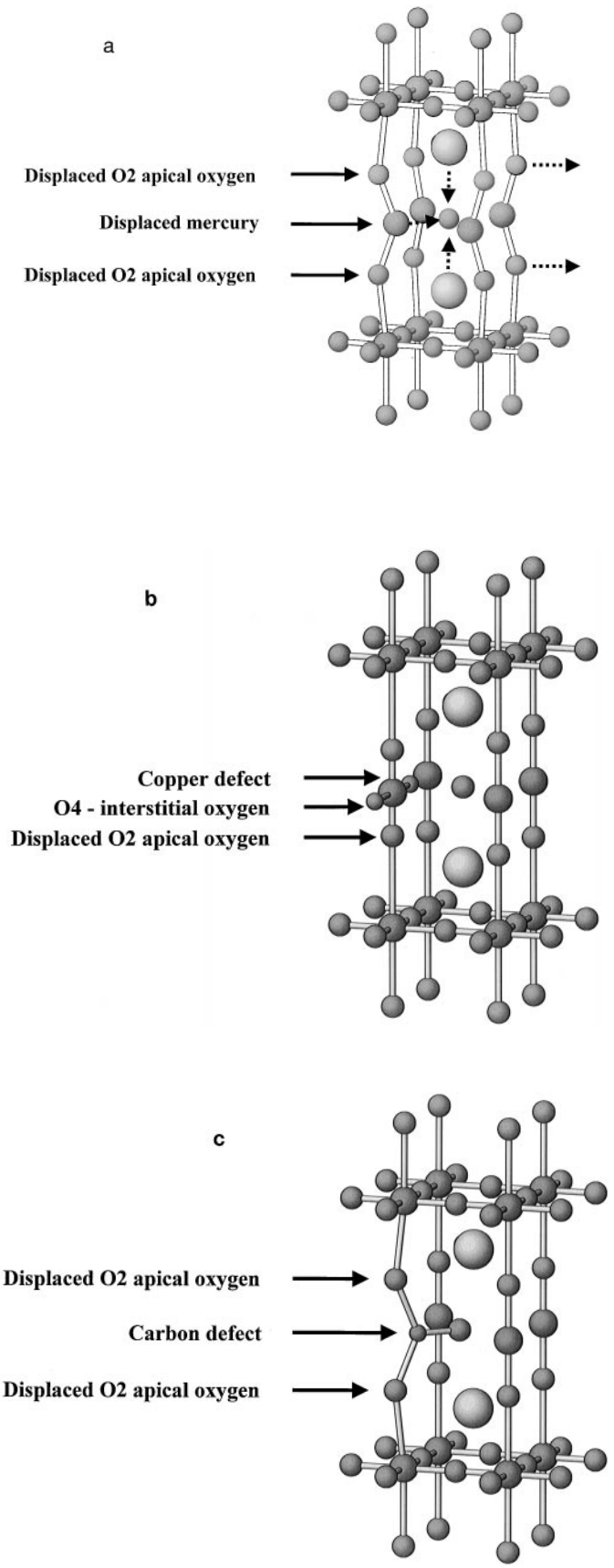

a split apical O2 position to satisfy the respective bonding requirements of both the mercury atom and the copper, or carbonate, substituent. In addition, in the case of partial carbonate substitution, significant displacement of the O2 oxygen away from the $(0,0,z)$ position to a new (x,x,z) position to accommodate the trigonal coordination of carbon as the CO_3^{2-} carbonate unit, would be anticipated (see Fig. 2c). In either case, inappropriate modeling of such displacements will be manifest in high isotropic thermal parameters for O2 oxygen.

Of these crystal defects, only the partial substitution of mercury by copper has been unambiguously determined and has been the subject of a number of studies (3, 8, 9). In these investigations, there is evidence for an additional oxygen site, associated with the copper substituent, located near the $(0,\frac{1}{2},0)$ position (designated the interstitial O4 oxygen site), as shown in Fig. 2b. However, although the precise nature of the coupled Cu–O4 defect is uncertain, there is general agreement on the basis of previous single-crystal X-ray diffraction (9) and powder neutron diffraction studies (3, 8), that the partial substitution of Hg by Cu appears coincident with the partial occupation of the O4 site.

The case of partial carbonate substitution for Hg is perhaps less well established, however. It is noteworthy that powder neutron diffraction studies which have pointed to such a defect have generally been carried out using samples prepared by high-pressure methods (5, 10). This suggests that the high-pressure synthesis route may be effective in stabilizing the partial substitution of linear HgO_2^{2-} units by CO_3^{2-} species, a process that may not be thermodynamically favored at room pressure. Indeed, it is pertinent to note that high-pressure methods are deemed *essential* for the synthesis of complex copper oxycarbonate superconductors (containing discrete CO_3^{2-} layers). Since the sample described in this study was prepared by a *room pressure* solid state reaction, we will make no further mention of carbonate substitution for Hg in connection with the present study. We will return to consider the issue of partial substitution of Hg by Cu.

Both powder neutron diffraction (6) and single-crystal X-ray diffraction studies (7, 11) have indicated the possibility of static displacements of Hg, Ba, and the O2 oxygen induced by occupation of the O3 position in the HgO_δ plane. On the basis of electrostatic arguments, one might expect the neighboring Hg and Ba atoms to be displaced toward the O3 interstitial, as illustrated schematically in Fig. 2a. Such a model effectively results in three coordinate

FIG. 2. (a) Schematic representation of possible static atomic displacements (indicated by broken arrows) in $HgBa_2CuO_{4+\delta}$. (b) Schematic representation of partial Cu substitution for Hg, coupled with occupation of the interstitial O4 oxygen position, in $HgBa_2CuO_{4+\delta}$. (c) Schematic representation of partial substitution of Hg by carbonate species in $HgBa_2CuO_{4+\delta}$.

Hg and nine coordinate Ba in the *defect unit cell* (in which the O3 position is occupied) with respect to eight coordinate Ba in the *conventional unit cell* (in which the O3 position is vacant). Furthermore, one should also expect the displacement of the O2 oxygens away from the Hg and Ba atoms, in order to satisfy the local chemical bonding requirements for these species, as shown in Fig. 2a.

We have undertaken a comprehensive study of the crystal structure of $HgBa_2CuO_{4+\delta}$ in order to resolve the issue of partial substitution of mercury by copper, and to examine the possibility of static atom displacements induced by the occupation of the interstitial O3 site. We present here the results of conjoint powder neutron and X-ray diffraction studies of $HgBa_2CuO_{4+\delta}$ which provide evidence for static displacements of the Hg cation and O2 oxygen away from their ideal positions, induced by the occupation of the interstitial O3 site.

EXPERIMENTAL

Synthesis of $HgBa_2CuO_{4+\delta}$

Polycrystalline samples of $HgBa_2CuO_{4+\delta}$ were prepared by a room pressure solid state reaction from stoichiometric quantities of HgO and $Ba_2CuO_{3+\delta}$. The synthesis of $Ba_2CuO_{3+\delta}$ was achieved from stoichiometric quantities of BaO_2 and CuO. An intimate mixture of these reagents was heated at 930°C, under flowing oxygen for 48 h and slow-cooled to room temperature at a rate of 30°C/h, with one intermittent grinding. Since $Ba_2CuO_{3+\delta}$ undergoes facile degradation in the presence of atmospheric CO_2 and moisture, this pecursor was immediately transferred to an argon-filled glove box, where it was combined with a stoichiometric amount of HgO. This mixture was pelletized, the pellets wrapped in silver foil, and subsequently sealed in a quartz ampoule containing air at 1 bar pressure. The quartz ampoule contained in a steel reaction-bomb, was heated to 750°C in 4 h, held at this reaction temperature for 8 h, and subsequently quenched in air to room temperature.

Superconducting Properties

The superconducting properties of the as-prepared sample of $HgBa_2CuO_{4+\delta}$ were analyzed using a Cryogenics S100 d.c.-SQUID susceptometer. The sample was measured under zero field and field cooled conditions, using an applied magnetic field of 2 G.

Powder X-Ray Diffraction Studies

Powder X-ray diffraction data were collected on a Siemens D5000 diffractometer, using Cu$K\alpha_1$ radiation (selected by a primary beam Ge monochromator). This instrument operates in para-focussing geometry and is fitted with a Position Sensitive Detector. For Rietveld profile analysis, diffraction data were acquired over the angular range $5 \leq 2\theta \leq 100°$, using a step size of 0.02°. The raw diffraction data were corrected for sample absorption, due to the relatively high mass absorption coefficients of Ba and Hg (325 $cm^2\,g^{-1}$ and 188 $cm^2\,g^{-1}$, respectively, for Cu$K\alpha$ radiation (12)).

Time-of-Flight Powder Neutron Diffraction Studies

Time-of-flight powder neutron diffraction studies on $HgBa_2CuO_{4+\delta}$ were performed using the high intensity, medium resolution, POLARIS diffractometer at the ISIS facility at the Rutherford Appleton Laboratory, with the sample contained in cylindrical vanadium can. For the purpose of Rietveld profile analysis, data from the high-resolution c-bank detectors ($135° < 2\theta < 160°$) were analyzed. The raw data were corrected for sample attenuation, due to the high neutron absorption coefficient of Hg ($\sigma_b = 372.3$ barns) (13).

Rietveld Profile Analysis

Rietveld profile analysis was performed using the GSAS suite of programs (14). For powder X-ray diffraction data, the reflection profiles were modeled using a pseudo-Voigt function and the background was modeled using a linear interpolation function. For time-of-flight powder neutron diffraction data, the reflection profiles were modeled using a convolution of back-to-back exponentials and a pseudo-Voigt function (of the Ikeda–Carpenter type), with the background modeled using a linear interpolation function. A small region (13.0–13.4 μs) of the time-of-flight powder neutron diffraction data was excluded from the Rietveld profile analysis, due to the presence of a small Bragg reflection originating from the vanadium can used to contain the sample.

RESULTS AND DISCUSSION

For the purpose of our combined powder neutron and X-ray diffraction study, a single-phase sample of mass $\sim$2 g was prepared. The X-ray powder diffraction pattern, shown in Fig. 3, confirms the single-phase nature of this sample. The lattice parameters of this sample were determined as $a = 3.8779(5)$ Å and $c = 9.5048(11)$ Å. These lattice parameters are in excellent agreement with those initially reported by Putilin *et al.* (1), and those reported by other groups in Table 1.

The temperature dependence of the magnetic susceptibility of the $\sim$2g sample (under field cooled conditions), is given in Fig. 4. This shows a sharp superconducting transition at $T_c = 96$ K, characterized by the onset of diamagnetism. This is very close to the optimum $T_c = 97$ K

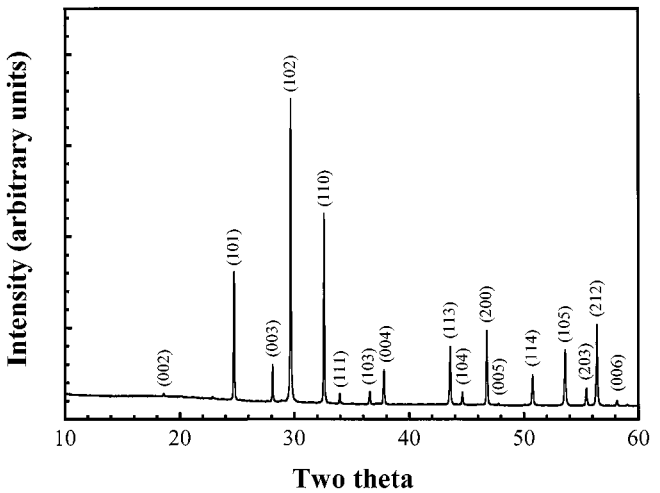

FIG. 3. Powder X-ray diffraction pattern of $HgBa_2CuO_{4+\delta}$.

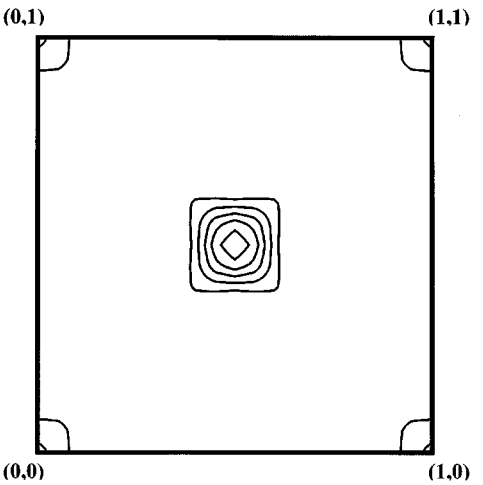

FIG. 5. Difference Fourier map ($F_{obs} - F_{calc}$) generated for the (x, y, 0) section of $HgBa_2CuO_{4+\delta}$. The O3 oxygen was excluded from the calculation of F_{calc}; contours are drawn at intervals of 0.314 fmÅ^{-3}.

(1–3) reported for $HgBa_2CuO_{4+\delta}$. The Meissner fraction at 10 K is estimated to be $\sim$75%, without correction for demagnetization effects.

Rietveld profile analysis of the time-of-flight powder neutron diffraction data was undertaken assuming the space group $P4/mmm$, and incorporating the lattice parameters determined from powder X-ray diffraction data (detailed above); the initial atom coordinates were those reported by Putilin *et al.* (1). The first stage of the refinement process did not include the interstitial O3 $(\frac{1}{2},\frac{1}{2},0)$ or O4 $(0,\frac{1}{2},0)$ oxygen sites. The scale factor, background, reflection profiles, lattice parameters, atom positions, and individual thermal parameters were refined. The refinement converged to give a satisfactory fit to the data, with $R_p = 3.79\%$, $R_{wp} = 2.02\%$, and $\chi^2 = 2.37\%$. In order to identify the interstitial oxygen sites in the HgO_δ plane, a difference Fourier map was generated for the (x, y, 0) section. This section, shown in Fig. 5, indicates a prominent maximum in nuclear density centered at the $(\frac{1}{2},\frac{1}{2},0)$ position, corresponding to the O3 interstitial oxygen site. The difference Fourier map did not reveal the presence of any significant nuclear density near the $(0,\frac{1}{2},0)$ position, corresponding to the O4 oxygen site, suggesting that the occupancy of this position is negligible in the sample studied here.

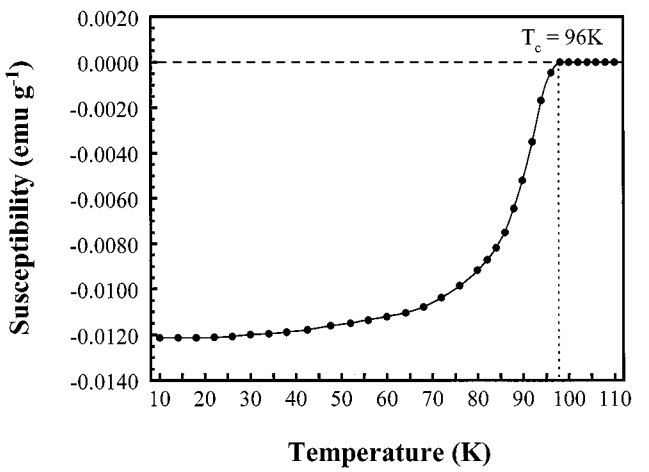

FIG. 4. Temperature dependence of magnetic susceptibility of $HgBa_2CuO_{4+\delta}$, showing an onset $T_c = 96$ K.

The O3 site was subsequently included in the structural model and the fractional occupancy and isotropic thermal parameter of this interstitial oxygen allowed to refine. The refinement converged smoothly, leading to an improved fit with $R_p = 3.60\%$, $R_{wp} = 1.93\%$, and $\chi^2 = 2.15\%$. The final positional and thermal parameters are summarized in Table 2.

The data summarized in Table 2 are in good agreement with those reported from other powder neutron diffraction studies (assembled in Table 1). The partial occupancy of the O3 interstitial position was determined to be 0.09(1), consistent with previous studies (c.f. Table 1). From Eq. [1], using the value of $\delta = 0.09$ determined from the powder neutron diffraction study, we calculate an expected $T_c = 97$ K, very close to that determined from SQUID susceptometry.

Interestingly, in accordance with the data presented in Table 1, large isotropic thermal parameters associated with the Hg and O2 atoms are observed in the present study. This may be symptomatic of partial substitution of Hg by Cu, or alternatively static displacement of the Hg and O2 atoms away from their ideal positions. The absence of

TABLE 2
Structural Parameters for $HgBa_2CuO_{4+\delta}$, Derived from Powder Neutron Diffraction Data

Space group: *P*4/*mmm*
Lattice parameters: $a = 3.8755(1)$ Å $c = 9.4994(1)$ Å
Powder statistics: $R_p = 3.60\%$[a] $R_{wp} = 1.93\%$[b] $\chi^2 = 2.15\%$[c]

Atom	Site	x	y	z	n	B_{iso} (Å^2)
Hg	1(*a*)	0	0	0	1	1.0(1)
Ba	2(*h*)	$\frac{1}{2}$	$\frac{1}{2}$	0.2980(1)	1	0.4(1)
Cu	1(*b*)	0	0	$\frac{1}{2}$	1	0.1(1)
O1	2(*e*)	$\frac{1}{2}$	0.0	$\frac{1}{2}$	1	0.3(1)
O2	2(*g*)	0	0	0.2083(1)	1	1.0(1)
O3	1(*c*)	$\frac{1}{2}$	$\frac{1}{2}$	0	0.09(1)	1.1(1)

[a] $R_p = \dfrac{\sum|(Yi(\text{obs}) - (1/c)\,Yi(\text{calc}))|}{\sum Yi(\text{obs})}$.

[b] $R_{wp} = \left[\dfrac{\sum|(wi(Yi(\text{obs}) - (1/c)\,Yi(\text{calc})))^2|}{wi\sum Yi(\text{obs})^2}\right]^{1/2}$.

[c] $R_{exp} = \dfrac{R_{wp}}{\sqrt{\chi^2}}$.

TABLE 3
Structural Parameters for $HgBa_2CuO_{4+\delta}$ Derived from Powder X-Ray Diffraction Data

Space group: *P*4/*mmm*
Lattice parameters: $a = 3.8777(1)$ Å $c = 9.5054(1)$ Å
Powder statistics: $R_p = 2.86\%$ $R_{wp} = 3.79\%$ $\chi^2 = 4.92\%$

Atom	Site	x	y	z	n	B_{iso} (Å^2)
Hg	1(*a*)	0	0	0	1	2.2(1)
Ba	2(*h*)	$\frac{1}{2}$	$\frac{1}{2}$	0.2984(1)	1	1.6(1)
Cu	1(*b*)	0	0	$\frac{1}{2}$	1	1.3(1)
O1	2(*e*)	$\frac{1}{2}$	0.0	$\frac{1}{2}$	1	0.8(1)
O2	2(*g*)	0	0	0.2100(5)	1	2.1(1)
O3	1(*c*)	$\frac{1}{2}$	$\frac{1}{2}$	0	0.09	1.1

significant nuclear density at the O4 position, as revealed by difference Fourier methods, suggests that the partial substitution of Hg by Cu in the present sample is unlikely, since the proposed substitutional defect is generally considered to be coupled with the occupation of the O4 site (3, 8, 9). In order to resolve the question of Cu substitution for Hg at the (0, 0, 0) position, a powder X-ray diffraction study was performed on this sample. The large difference in scattering power of Hg and Cu, with respect to X-rays, enables one to reliably assess the possibility of partial substitution of Hg by Cu via this diffraction technique.

The initial crystallographic parameters for the powder X-ray diffraction study were those resulting from the time-of-flight powder neutron diffraction study and are summarized in Table 2. Initially, no substitution of Cu for Hg was assumed; the scale factor, background, reflection profiles, lattice parameters, atom positions, and individual thermal parameters were refined. However, the occupancy of the O3 position was maintained at $n = 0.09$ and the corresponding thermal parameter was fixed at $B_{iso} = 1.1$ Å^2, as determined from the powder neutron diffraction study. We consider this appropriate, given the superior precision of powder neutron diffraction over powder X-ray diffraction in the determination of the partial occupancy of the O3 position. The refinement converged, giving a satisfactory fit to the powder X-ray diffraction data, with $R_p = 2.86\%$, $R_{wp} = 3.79\%$, and $\chi^2 = 4.92\%$, the final positional and thermal parameters are summarized in Table 3 and the final profile fit is shown in Fig. 6.

The possibility of partial substitution of Cu for Hg was then examined by allowing for a mixed Hg/Cu site at the (0, 0, 0) position. The fraction of Hg and Cu atoms at that position was constrained to sum to unity, and the thermal parameters of the Hg and Cu atoms were constrained to be equal. Subject to these constraints, a refined occupancy of 0.003(5) was determined for Cu, with the remaining structural parameters essentially unchanged from those reported in Table 3. Since the refined occupancy of Cu is within the estimated standard deviation, we conclude that the (0, 0, 0) position is occupied exclusively by Hg in the current sample. This is in accord with the absence of significant *nuclear* density at the O4 position, revealed by difference Fourier methods. Partial occupancy of the O4 position would be expected in the case of partial substitution of Cu at the Hg site, given the general consensus on the coupled nature of the Cu–O4 defect (3, 8, 9).

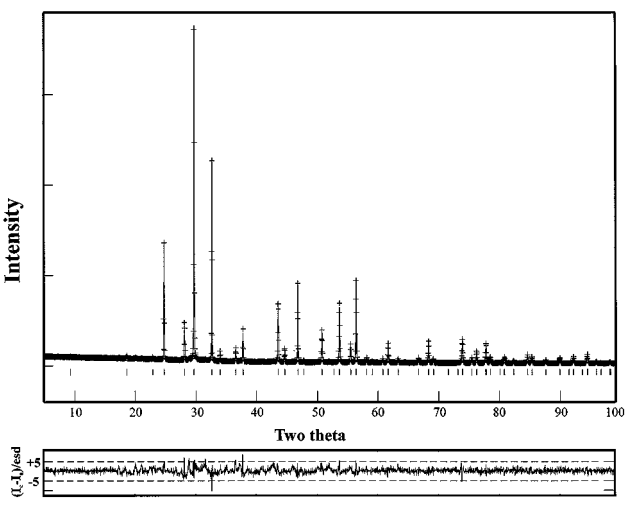

FIG. 6. Final profile fit (solid line) to powder X-ray diffraction data (+) for $HgBa_2CuO_{4+\delta}$, the difference/esd profile is shown below. The tick marks show the positions of the Bragg reflections.

Since we have effectively excluded the possibility of partial substitution of Hg by Cu in the present sample, we now turn to consider the possibility that the large thermal parameters characteristic of the Hg and O2 atoms may be symptomatic of static displacements of these atoms away from their ideal positions. As discussed in the Introduction, occupation of the O3 position would be expected to attract the neighboring Hg and Ba atoms, with a concomitant displacement of the neighboring O2 oxygens, in order to maintain the appropriate chemical bonding requirements of Hg and Ba. To examine the possibility of such static displacements, further analysis of the time-of-flight powder neutron diffraction data was undertaken. Refinement of anisotropic thermal parameters for the Hg, Ba, and O2 atoms, yielded distorted thermal ellipsoids, in accordance with the previous hypothesis: for Hg, $B_{11} = 1.1(1)$ Å^2, $B_{33} = 0.7(1)$ Å^2; for Ba, $B_{11} = 0.2(1)$ Å^2 and $B_{33} = 0.9(1)$ Å^2; and for O2, $B_{11} = 1.2(1)$ Å^2, $B_{33} = 0.7(1)$ Å^2. The anisotropic thermal parameters are relatively large, in comparison with the isotropic thermal parameters, given in Table 2, suggesting some static displacement of the Hg and O2 atoms in the x, y-plane, and of Ba along the z direction, in accordance with the previous hypothesis on the basis of simple electrostatic arguments.

In order to investigate the proposed static displacements using the powder neutron diffraction data, a modified structural model was devised in which the fraction of displaced atoms was coupled with the fractional occupancy of the O3 position. For a fraction n of occupied O3 positions, one expects the displacement of $4n$ Hg atoms, $2n$ Ba atoms, and $8n$ O2 atoms. Thus, the modified structural model is a convolution of $1 - n$ *conventional cells*, in which the O3 site is vacant and there are *no* static displacements of the Hg, Ba, and O2 atoms, and n *defect cells*, in which the O3 position is occupied and the proposed displacements occur *exclusively*.

Initially, the displacement of only the Hg and O2 atoms was considered. The Hg and O2 positions were thus split to yield displaced atoms, at Hg′ (x, x, 0) and O2′ (x, x, z) having initial occupancies of $4n$ and $8n$, respectively, with $n = 0.09$ as determined previously (see Table 2). The occupancies of the Hg′ and O2′ sites were constrained to be equal to $4n$ and $8n$, respectively, with the sum of the occupancies of the Hg and Hg′, and O2 and O2′ atoms constrained to unity. In addition, the z coordinates of the O2 and O2′ atoms were constrained to be identical. The isotropic thermal parameters of the Hg and Hg′ and O2 and O2′ atoms were constrained to be equal.

On the basis of the modified structural model, and subject to the constraints described above, the refinement converged to yield a significantly improved fit to the powder neutron diffraction data, with $R_p = 3.57\%$, $R_{wp} = 1.78\%$, and $\chi^2 = 1.85\%$. The structural model was then adjusted to allow, first, for the displacement of the Ba atom toward the O3 interstitial, and second for independent z coordinates for the O2 and O2′ atoms, in order to reflect the different z coordinates of the Ba and Ba′ atoms. However, no significant displacement of these atoms from their "parent" positions, could be ascertained. The final structural model, therefore, incorporated only split Hg and O2 positions, with the split oxygen atoms constrained to have the same z coordinate. The final positional and thermal parameters are summarized in Table 4 and the final profile fit is shown in Fig. 7.

TABLE 4

Structural Parameters for $HgBa_2CuO_{4+\delta}$ Allowing for Displacement of Hg and O2 Atoms; Derived from Powder Neutron Diffraction Data

Space group:	$P4/mmm$			
Lattice parameters:	$a = 3.8757(1)$ Å	$c = 9.4998(1)$ Å		
Powder statistics:	$R_p = 3.57\%$	$R_{wp} = 1.78\%$	$\chi^2 = 1.85\%$	

Atom	Site	x	y	z	n	B_{iso} (Å^2)
Hg	1(a)	0	0	0	0.72(1)	0.7(1)
Hg′	4(j)	0.031(2)	0.031(2)	0	0.07(1)	0.7(1)
Ba	2(h)	0.5	0.5	0.2980(1)	1	0.4(1)
Cu	1(b)	0	0	0.5	1	0.1(1)
O1	2(e)	0.5	0.0	0.5	1	0.3(1)
O2	2(g)	0	0	0.2085(1)	0.72(1)	0.6(1)
O2′	8(r)	0.045(2)	0.045(2)	0.2085(1)	0.07(1)	0.6(1)
O3	1(c)	0.5	0.5	0	0.07(1)	0.6(1)

Note. Constraints: $n(Hg') = 4n(O3)$; $n(O2') = 8n(O3)$; $n(Hg) + n(Hg') = 1$; $n(O2) + n(O2') = 1$; $z(O2') = z(O2)$; $B_{iso}(Hg') = B_{iso}(Hg)$; $B_{iso}(O2') = B_{iso}(O2)$.

Thus, allowing for static displacements of the Hg and O2 atoms away from their "ideal" positions, leads to an improved fit to the powder neutron diffraction data. The occupancy of the interstitial oxygen position at $(\frac{1}{2}, \frac{1}{2}, 0)$ was

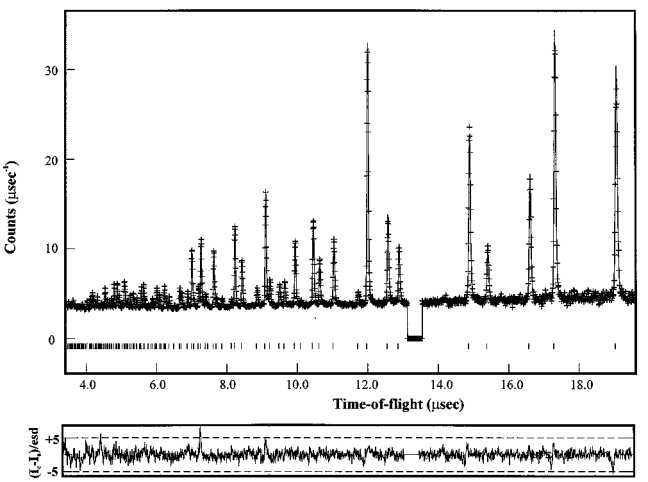

FIG. 7. Final profile fit (solid line) to time-of-flight powder neutron diffraction data (+) for $HgBa_2CuO_{4+\delta}$, the difference/esd profile is shown below. The tick marks show the positions of the Bragg reflections.

TABLE 5
Selected Bond Lengths and Bond Angles for the Conventional and Defect Unit Cells in $HgBa_2CuO_{4+\delta}$ Determined from Time-of-Flight Neutron Diffraction Data

Conventional cell		Defect cell	
Hg–O2	1.981(1) Å	Hg′–O2′	2.023(3) Å
		Hg–O3	2.573(1) Å
Ba–O1	2.727(1) Å	Ba–O1	2.727(1) Å
Ba–O2	2.869(1) Å	Ba–O2′	3.103(11) Å
		Ba–O3	2.830(1) Å
Cu–O1	1.938(1) Å	Cu–O1	1.938(1) Å
Cu–O2	2.769(1) Å	Cu–O2′	2.779(2) Å
O2–Hg–O2	180°	O2′–Hg′–O2′	170.5(5)°
O1–Cu–O2	90°	O1–Cu–O2′	82.9(5)°

found to be 0.07(1), corresponding to a nominal copper valence of $Cu^{2.14+}$. On the basis of our Rietveld profile analysis, we observe the displacement of Hg and O2 atoms by 0.16 and 0.25 Å, respectively, in the (110) direction, away from their ideal positions. Table 5 compares selected bond lengths and bond angles for the conventional and defect unit cells based on the crystallographic data summarized in Table 4.

If we allow for the displacement of Hg and O2 atoms away from their ideal positions, the Hg–O2 bond length increases from 1.981 to 2.023 Å, with a concomitant reduction in the O2–Hg–O2 bond angle from 180° to 170.5°. Notably, the Hg′–O3 bond length of 2.573 Å, is much longer than the Hg′–O2′ bond length in the defect cell, suggesting that the Hg′–O3 bonds is of a very different nature in comparison with the Hg′–O2′ bond. It is interesting to compare these bond lengths with those observed in HgO (15). In this binary oxide one observes infinite chains composed of HgO_2 "dumb-bells' akin to those observed in the mercurocuprates, as shown in Fig. 8. Strong *intra*chain bonding is observed, with an intrachain Hg–O bond length of 2.03 Å; *inter*chain bonding is weaker, with an interchain Hg–O bond length of 2.80 Å. In Fig. 8 we show the structure of HgO highlighting the shorter intrachain Hg–O bonds, the longer interchain bonds (omitted for clarity) cross-link the infinite Hg–O chains. In the defect cell of $HgBa_2CuO_{4+\delta}$, the Hg–O2′ bond length (2.023 Å) is very close to the intrachain Hg–O bond length in HgO, whereas the longer Hg–O3 bond length (2.573 Å) is somewhat shorter than the interchain bond length. This suggests the nature of the Hg–O2 bond in the mercurocuprates is analogous to the strong intrachain bond in HgO, whereas the nature of the Hg–O3 bond is more akin to the weaker interchain bond found in HgO.

Within $HgBa_2CuO_{4+\delta}$ the displacement of the O2 atoms occurs in the opposite direction to that of the Hg atoms, along the (110) vector. This displacement occurs to allow for

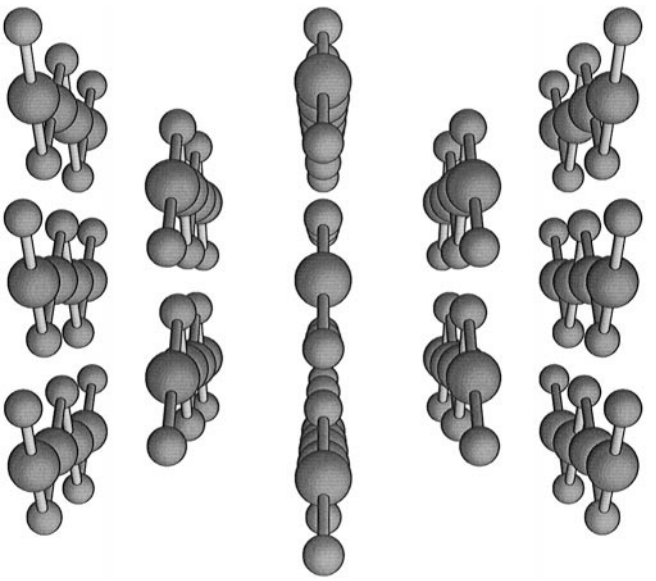

FIG. 8. The structure of HgO illustrating the linking of HgO_2 dumbells to form infinite chains.

the increase in coordination number of Hg and Ba in the defect unit cell, relative to the conventional cell in which the O3 site is vacant. This is inferred from bond valence sums calculated (according to the scheme of Brown and Altermatt (16, 17)) for the Hg, Ba, and Cu atoms in the conventional and defect unit cells summarized in Table 6, based on the data in Tables 4 and 5. The displacement of the O2 atoms allows the Hg atom to maintain a bond valence sum of $\sim 1.95+$ in the defect cell, although the coordination number of this atom has effectively increased from two to three, relative to the conventional cell. The bond valence sum of the Ba atom is calculated to be $2.03+$ in the conventional cell, whereas the bond valence sum for the Ba′ atom in the defect cell is $1.90+$. This indicates that the displacement of the O2 atoms in the (110) direction in the defect cell occurs to allow for an increase in the coordination number of the Ba atom, from eight in the conventional cell to nine in the defect cell, due to the additional oxygen at the O3 site in the latter. The calculated bond valence for the Ba atom in the defect cell is somewhat lower than expected, which may

TABLE 6
Bond Valence Sums Calculated for the Conventional and Defect Unit Cells in $HgBa_2CuO_{4+\delta}$

Ion	Conventional cell	Defect cell
Hg	1.95+	1.94+
Ba	2.03+	1.90+
Cu	2.10+	2.10+

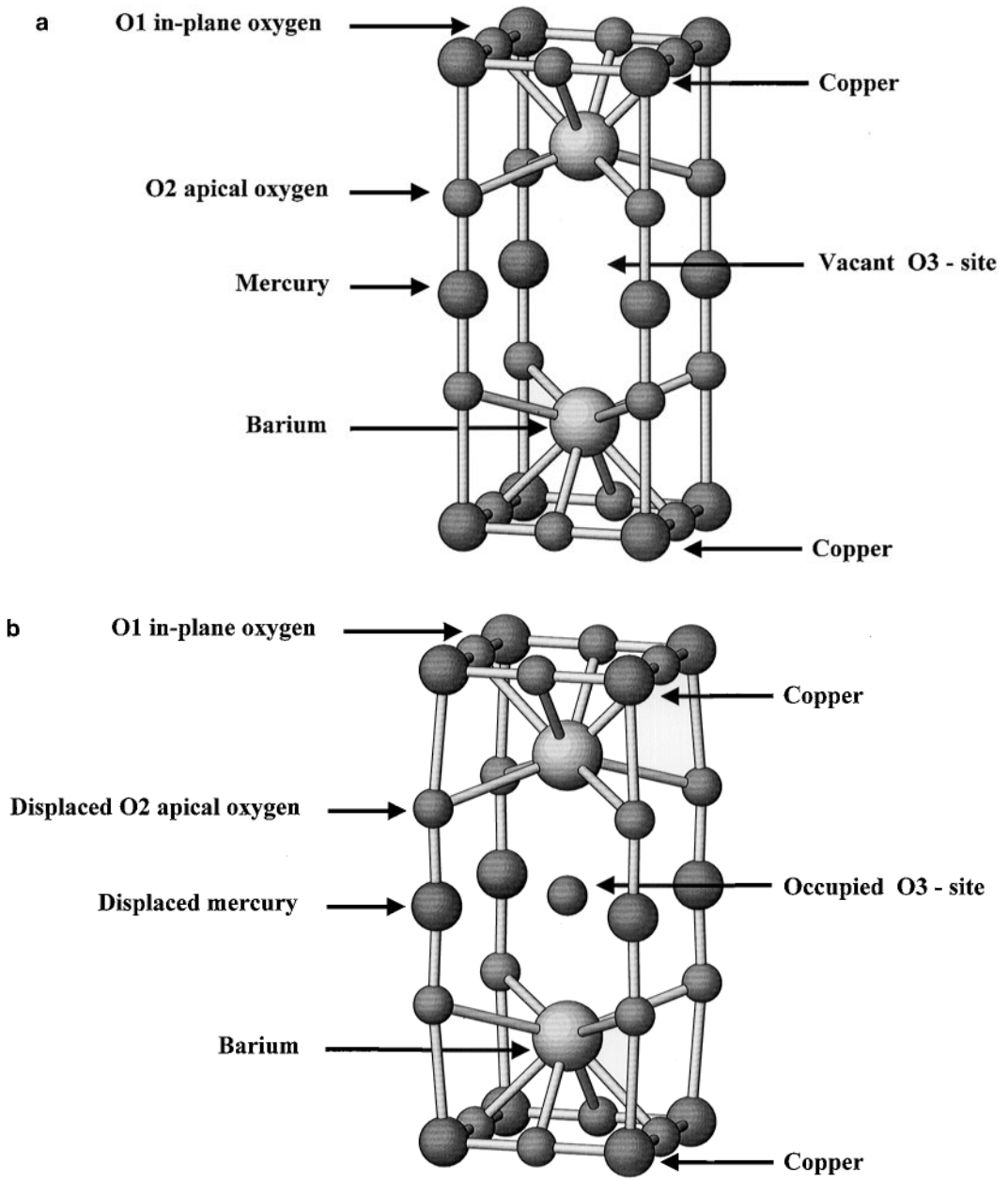

FIG. 9. (a) The crystal structure of the "conventional cell" in $HgBa_2CuO_{4+\delta}$, determined from analysis of time-of-flight powder neutron diffraction data. Note the vacant O3 site in this unit cell. (b) The crystal structure of the "defect cell" in $HgBa_2CuO_{4+\delta}$, determined from analysis of time-of-flight powder neutron diffraction data. Note the static atomic displacements induced by occupation of the O3 site in this unit cell.

be due to the fact that we could not account for the proposed static displacement of the Ba atom toward the O3 interstitial in the defect cell. Such a displacement would be expected to lead to an increase the bond valence sum of the Ba′ atom. Since we have been unable to resolve the displacement of the Ba cation in the defect cell in the current experiment, we conclude that the magnitude of this static displacement must be small. Finally, it should be noted that the displacement of the O2 atoms in the (110) direction leads to an increased Cu–O2 bond length in the defect cell, and a reduction in the O1–Cu–O2 bond angle, relative to the conventional cell, while maintaining a sensible bond valence sum of 2.10 + for copper.

In general terms, the crystal structures of the conventional and defect unit cells are very similar. The full magnitude of the crystallographic displacements in the defect cell is clearly apparent, when compared with the undistorted conventional cell, as shown in Figs. 9a and 9b. The defect

cell appears considerably warped, in comparison with the conventional cell, due to the displacement of the O2 atoms to allow for the increase in coordination number for Hg and Ba.

The static displacement of Hg and O2 atoms in $HgBa_2CuO_{4+\delta}$ reported here has also been proposed on the basis of computational methods, in the higher homologues $HgBa_2CaCu_2O_{6+\delta}$ and $HgBa_2Ca_2Cu_3O_{8+\delta}$. Zhang *et al.* (18), have reported that the Hg and Ba atoms are displaced by 0.12 and 0.17 Å in the (110) and *z* directions, respectively, toward the interstitial oxygen position in the HgO_δ plane, in $HgBa_2CaCu_2O_{6+\delta}$. The O2 atoms are calculated to move 0.22 Å in the opposite direction to the Hg atoms, along the (110) vector. In the case of $HgBa_2Ca_2Cu_3O_{8+\delta}$, Islam and Winch (19) have reported the displacement of the Hg and Ba atoms by 0.6 and 0.1 Å in the (110) and *z* directions, respectively, toward the interstitial oxygen. The displacements of the Hg and O2 atoms observed in the present study are in remarkably good agreement with those calculated by atomistic computer simulation techniques for $HgBa_2CaCu_2O_{6+\delta}$ (18), although we have not been able to discern any significant displacement of the Ba atom from its ideal position.

Recently, a high-pressure powder synchrotron X-ray diffraction study of $HgBa_2CaCu_2O_{6+\delta}$ and $HgBa_2Ca_2Cu_3O_{8+\delta}$ has proposed a reversible phase transition in these materials, at $\sim$24 and 15 GPa, respectively, due to pressure induced ordering of the interstitial oxygen atoms (20). Given the significant magnitude of the crystallographic relaxation around the interstitial oxygen defect in the HgO_δ plane of the mercurocuprates (reported both here and in the aforementioned computational studies) it is highly likely that the observed ordering of the interstitial oxygen under conditions of high pressure may indeed occur to minimise the free energy associated with such crystallographic distortions.

CONCLUSIONS

We have demonstrated, on the basis of time-of-flight powder neutron diffraction data, that significant static displacements of the Hg and O2 atoms occur in $HgBa_2CuO_{4+\delta}$, induced by the presence of interstitial oxygen atoms in the HgO_δ plane. The substitution of Hg by Cu, and the presence of a coupled Cu–O4 defect in the sample studied here has been ruled out by a powder X-ray diffraction study, and the absence of any significant nuclear density near the $(0, \frac{1}{2}, 0)$ position in difference Fourier maps calculated on the basis of powder neutron diffraction data. The role of the interstitial oxygen in determining the superconducting properties of the mercury-based superconductors has been well documented. However, as we have illustrated here, the effect of the interstitial oxygen on the local crystallographic environment in these materials, is equally profound.

ACKNOWLEDGMENTS

We are grateful to Merck Ltd. and the EPSRC for the provision of a CASE studentship for N.C.H. We thank Dr. J. A. Hriljac, Dr. Y. Miyazaki, and Professor R. B. Von Dreele for useful discussions during the course of this study.

REFERENCES

1. S. N. Putilin, E. V. Antipov, O. Chmaissem, and M. Marezio, *Nature* **362,** 226 (1993).
2. P. P. Edwards, G. B. Peacock, J. P. Hodges, A. Asab, and I. Gameson, *in* "High Temperature Superconductivity 1996: 10 Years After the Discovery" (E. Kaldis, E. Liarokapis and K. A. Müller, Eds.), Kluwer Academic, Dordrecht, 1997.
3. A. Asab, A. R. Armstrong, I. Gameson, and P. P. Edwards, *Physica C* **255,** 180 (1995).
4. O. Chmaissem, Q. Huang, S. N. Putilin, M. Marezio, and A. Santoro, *Physica C* **212,** 259 (1993).
5. S. M. Louerio, E. T. Alexandre, E. V. Antipov, J. J. Capponi, S. de Brion, B. Souletie, J. L. Tholence, M. Marezio, Q. Huang, and A. Santoro, *Physica C* **243,** 1 (1995).
6. Q. Huang, J. W. Lynn, Q. Xiong, and C. W. Chu, *Phys. Rev. B* **52,** 462 (1995).
7. Bertinotti, V. Viallet, D. Colson, J.-F. Marucco, J. Hammann, G. Le Bras, and A. Forget, *Physica C* **268,** 257 (1996).
8. J. L. Wagner, P. G. Radaelli, D. G. Hinks, J. D. Jorgensen, J. F. Mitchell, B. Dabrowski, G. S. Knapp, and M. A. Beno, *Physica C* **210,** 447 (1993).
9. D. Pelloquin, V. Hardy, A. Maignan, and B. Raveau, *Physica C* **273,** 205 (1997).
10. S. M. Louerio, E. V. Antipov, J. J. Capponi, and M. Marezio, *Mater. Res. Bull.* **30,** 1463 (1995).
11. P. Bordet, F. Duc, S. LeFloch, J. J. Capponi, E. Alexandre, M. Rosa-Nunes, S. Putilin, and E. V. Antipov, *Physica C* **271,** 189 (1996).
12. "International Tables for Crystallography: Volume C" (A. J. C. Wilson, Ed.). Kluwer Academic, Dordrecht, 1995.
13. V. F. Sears, *Neutron News* **3,** 26 (1992).
14. A. C. Larson and R. B. Von Dreele "GSAS—General Structure Analysis System." Rep. LA-UR-86-748, Los Alamos National Laboratory, Los Alamos, NM 87545, 1990.
15. K. Aurivillius, *Acta Chem. Scand.* **10,** 852 (1956).
16. I. D. Brown and D. Altermatt, *Acta Crystallogr. Sect. B* **41,** 244 (1985).
17. I. D. Brown, *J. Solid State Chem.* **82,** 122 (1989).
18. X. Zhang, S. Y. Xu, and C. K. Ong, *Physica C* **262,** 13 (1996).
19. M. S. Islam and L. J. Winch, *Phys. Rev. B* **52,** 10510 (1995).
20. R. Gatt, J. S. Olsen, L. Gerward, I. Bryntse, A. Kareiva, I. Panas, and L. G. Johansson, *Phys. Rev. B* **57,** 13922 (1998).